

**Characterizing complex networks using Entropy-degree diagrams:  
unveiling changes in functional brain connectivity  
induced by Ayahuasca**

A. Viol,<sup>1,2,\*</sup> Fernanda Palhano-Fontes,<sup>3</sup> Heloisa Onias,<sup>3</sup> Draulio  
B. de Araujo,<sup>3</sup> Philipp Hövel,<sup>4,2</sup> and G. M. Viswanathan<sup>5,6,†</sup>

<sup>1</sup>*Institute of Theoretical Physics, Technische Universität,  
Berlin, Hardenbergstraße 36, 10623 Berlin, Germany*

<sup>2</sup>*Bernstein Center for Computational Neuroscience Berlin,  
Humboldt-Universität zu Berlin, Philippstraße 13, 10115 Berlin, Germany*

<sup>3</sup>*Brain Institute, Universidade Federal do Rio Grande do Norte, 59078-970 Natal-RN, Brazil*

<sup>4</sup>*School of Mathematical Sciences, University College Cork, Western Road, Cork, Ireland*

<sup>5</sup>*Department of Physics, Universidade Federal do  
Rio Grande do Norte, 59078-970 Natal-RN, Brazil*

<sup>6</sup>*National Institute of Science and Technology of Complex Systems  
Universidade Federal do Rio Grande do Norte, 59078-970 Natal-RN, Brazil*

(Dated: September 28, 2018)

## Abstract

Open problems abound in the theory of complex networks, which has found successful application to diverse fields of science. With the aim of further advancing the understanding of the brain's functional connectivity, we propose to evaluate a network metric which we term the *geodesic entropy*. This entropy, in a way that can be made precise, quantifies the Shannon entropy of the distance distribution to a specific node from all other nodes. Measurements of geodesic entropy allow for the characterization of the structural information of a network that takes into account the distinct role of each node into the network topology. The measurement and characterization of this structural information has the potential to greatly improve our understanding of sustained activity and other emergent behaviors in networks, such as self-organized criticality sometimes seen in such contexts. We apply these concepts and methods to study the effects of how the psychedelic Ayahuasca affects the functional connectivity of the human brain. We show that the geodesic entropy is able to differentiate the functional networks of the human brain in two different states of consciousness in the resting state: (i) the ordinary waking state and (ii) a state altered by ingestion of the Ayahuasca. The entropy of the nodes of brain networks from subjects under the influence of Ayahuasca diverge significantly from those of the ordinary waking state. The functional brain networks from subjects in the altered state have, on average, a larger geodesic entropy compared to the ordinary state. We conclude that geodesic entropy is a useful tool for analyzing complex networks and discuss how and why it may bring even further valuable insights into the study of the human brain and other empirical networks.

---

\* aline.viol@bccn-berlin.de

† gandhi@fisica.ufrn.br

## I. INTRODUCTION

In the last few decades, new scientific fields have taken advantages of complex network approaches. This interest emerged, in part, by virtue of technological advances that generate new datasets in computational, social, biological, among others sciences. Examples include modern brain mapping techniques, such as functional magnetic resonance imaging (fMRI), that have provided previously inaccessible information about interaction patterns in the human brain [1]. The theory of complex networks has proven to be a crucial tool to understand the interactions and dynamics in large systems.

Attempts to characterize those new datasets bring up the challenge of extracting relevant features regarding the network’s structure. One of the main concerns is to identify the role of each node in the network and how the nodes cooperate to give rise to emergent behaviors. The majority of measurements that have been proposed in the last few decades allow the ranking of nodes’ importance by the number of connections, centrality, etc. [2–4].

Instead of ranking a node’s relative importance, we ask how the nodes contribute locally to the global connectivity of the network, with the aim of better understanding the individualize role played by each node in the network. We quantitatively describe these roles, as well as the structural information of the diversity of interactions between nodes. The nodes in a network interact with their neighbors and, indirectly, with the neighbors of neighbors; and also with more distant nodes with even greater “neighborhood radius” (Figure 1).

We aim to quantify the diversity of influences on a given node, of all other nodes over the whole network. For each node, we calculate the Shannon entropy functional [5] of the probability distribution of the geodesic distances between each node and all other nodes. We call this measurement *geodesic entropy*. Nodes with a great diversity of influences (i.e., with high geodesic entropy) may play an important role in, for example, to guarantee specialization of functional patterns. Besides, nodes with a low diversity of influences may guarantee constraints relevant to network robustness. The “fine tuning” of the distribution of distances, quantified by the Shannon entropy, may be a key to understanding how emergent behaviors arise.

We illustrate and apply our method to real network data. We use the geodesic entropy to analyze human brain functional networks under the influence of the psychedelic Ayahuasca – a brew from the Amazonian indigenous cultures that contains the serotonergic psychedelic

N, N-Dimethyltryptamine (DMT) and monoamine oxidase inhibitors (MAOi) [6].

Ayahuasca ingestion may cause deep changes in the cognition and perceptions, promoting substantial alterations in the sense of the reality and the self [7, 8]. According to the neural correlate hypothesis, we expect to find features on functional brain networks that can be correlated to this specific consciousness state. We evaluate the networks extracted from fMRI data acquired from the same group of subjects in two sections: before and 40 minutes after Ayahuasca intake. The geodesic entropy is able to identify a specific behavior for networks related to the psychedelic state of consciousness: the nodes of functional brain networks under Ayahuasca effects tend to have a greater geodesic entropy than the ordinary condition.

## II. METHODS

A complex network is a schematic representation of the relations (links) between elements (nodes) of a system with a nontrivial topology of interactions [9, 10]. Consider a non-weighted undirected network  $G(\nu, \xi)$ , where  $\nu$  is a set with  $N$  nodes and  $\xi$  is the set of links. It is represented numerically by a  $N \times N$  adjacency matrix  $A_{i,j}$ : if a pair of nodes  $i$  and  $j$  are connected, the matrix element is  $A_{i,j} = 1$  and  $A_{i,j} = 0$  otherwise. The nodes are connected if the elements that they represent share some kind of information or have mutual influences. The number of links that have each node is termed degree. The statistics of the degrees in a network is quantified by the degree distribution, a histogram of degrees considering the whole network [9].

Nodes directly connected are called first neighbors. A node can also influence and be influenced by the neighbors of its neighbors, called second neighbors. Considering a connected network, the influences may be extended to all neighborhood radius. Our goal is to quantify the amount of information involved in the diversity of influence extending over the network. For this purpose, we calculated the Shannon entropy [5] considering the statistics of distances between a node and all their neighborhood radius.

Distances in network theory are related to the paths lengths. By definition, a path length  $\Gamma_{i,j}$  is the number of consecutive links between the pair of nodes  $i$  and  $j$ , following a specific trail. The shortest path length ( $D(i, j) = \min(\{\Gamma_{i,j}\})$ ) defines geodesic distance between two nodes [11]. The geodesic distance has been used in several network characterizations

such as small-world networks [12].

By looking at the distribution of geodesic distances for a given node, we can better understand the role played in the network by that particular node. Quantifying the diversity of influences due the geodesic distances brings to light the rules of how the information is distributed in the network.

We define  $P_i\{p_i(r), 1 \leq r \leq \max(D(i, \{j\}))\}$  as a probability mass function of find a node in the neighborhood ratio  $r$  of the node  $i$ . That is, the probability of, in a random choose, one selects a node  $j$  from the set of the remain nodes ( $\{j\} := j \in \nu / j \neq i$ ) with the geodesic distance  $D(i, j) = r$ . This probability is defined as:

$$p_i(r) = \frac{1}{(N-1)} \sum_{\{j\}} \delta_{D(i,j),r} ; \quad (1)$$

where neighborhood radius  $r$  assumes values according to the interval ( $1 \leq r \leq \max(D(i, \{j\}))$ ). See an illustration in Figure 1.

The distribution  $P_i(r)$  contains information about the connectivity across multiple links of a network. For illustration, consider hypercubic lattices of dimension  $D$  with links only between neighboring nodes. The distribution  $P_i(r)$  scales according to  $P_i(r) \sim r^{D-1}$ , because nodes a fixed distance  $r$  away lie on the (hyper)surface of constant distance to the node  $i$ , where in  $D$  dimensions, this surface has dimension  $D-1$ . Hence, it makes sense that the characterization of the distribution  $P_i(r)$  has the potential to provide insights into network connectivity.

The geodesic entropy is given by:

$$s_i^g[P_i] = - \sum_{r=1}^{r_{max}} p_i(r) \log p_i(r) ; \quad (2)$$

where  $r_{max} = \max(D(i, \{j\}))$ . The value of  $s_i^g$  does not depend on the network size for greater networks ( $N \gg r_{max}$ ). The characteristic geodesic entropy of a network is defined by:

$$S^g = \frac{1}{N} \sum_{i=1}^N s_i^g ; \quad (3)$$

Distinct from the entropy of the degree distribution, that quantifies the constraints imposed by the network degree distribution [13], the geodesic entropy quantifies the information due to the intrinsic configuration of network structure. Networks with different structures

can share the same degree distribution, that is, they can be degenerate in the entropy of the degree distribution. The characteristic geodesic entropy can lift the degeneracy of those networks. Besides, the geodesic entropy is a measurement more appropriate to characterize the nodes role and the underlying trends in the network topology.

We briefly compare and relate the geodesic entropy to similar quantities that have been used to study networks. The use of geodesic distances to evaluate Shannon entropy was firstly proposed by Chen and collaborators [14]. Instead define the entropy per node, they defined a global entropy ( $I_r(G)$ ) considering only one specific value  $r$  of geodesic distance. A recent work from Stella and Domenico proposes a similar formula proposed in this work to characterize centrality by mean of Shannon entropy [15]. Their proposes differente from ours by a normalization factor that depends on  $r_{max}$ . It limitates the entropy to be defined between 0 and 1. This normalization does not take in consideration the increase on entropy due the increase of maximum radius  $r_{max}$ . In contrast to the above methods, the geodesic entropy we propose here allows the evaluate the influence of the maximum neighborhood radius, as well as its dependence of network size, and to depict the role of each node in the network.

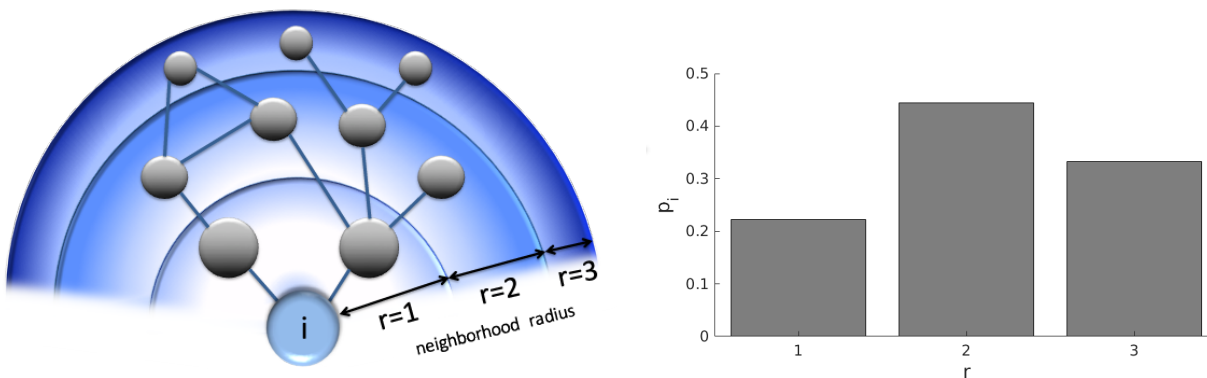


Figure 1. Schematic representation of neighborhood radius  $r$  and its probability distribution. The left panel shows three neighborhood radius for the node  $i$ . The nodes within the neighborhood  $r = 1$ ,  $r = 2$ ,  $r = 3$  are, respectively, 1, 2 and 3 links distant from the node  $i$ . On the right is the probability distribution of the geodesic distances for this network.

## A. Entropy-degree diagram

We introduce here the entropy-degree diagram, a viewer tool to help to map the role of nodes into the network. Entropy-degree diagram is built plotting the geodesic entropy ( $s_i^g$ ) versus the nodal degree  $k$  normalized by the maximum number of connections possible ( $k/(N - 1)$ ) for all nodes belonging to the network. This normalization allows we compare networks with different sizes. Figure 2 shows the entropy-degree diagram for 3 networks that share the same number of nodes and links, have the same degree distribution but have different structures. Each marker ( $\bullet$ ) represents a node. We used here colors as a didactic artifact to improve the visualization (it can be neglected to build the entropy-degree diagram). The colors are defined according to their maximum neighborhood radius ( $r_{max}$ ), that is, the greatest geodesic distance between the given node and the remaining nodes. The watermark regions follow the same colors and delimit the space of possibilities for each value of  $r_{max}$ . For example, the purple curve delimits the possible positions on the diagram for nodes with first and second neighbors. The region in blue delimits the positions for nodes with first, second and third neighbors and it follows for the others regions. The up limit of each  $r_{max}$  region are peaked at ( $k \approx 1/r_{max}$ ,  $s^g \approx \ln r_{max}$ ). Note the values have no dependence with the network size. They depend only on the network structure. The magnitude of the increment in the geodesic entropy due to the increase of  $r_{max}$  is inversely proportional to  $r_{max}$ , ( $\Delta s^g \approx r_{max}^{-1} \Delta r_{max}$ ). That means there is a limit in which the increase of maximum geodesic distances (increase the sparsity) contributes significantly to the network entropy. The lower limits will be affected by the size of the network and converge to the first curve ( $r_{max} = 2$ ) for large networks. See Figure 3. We would like to let open the question if it could explain some optimization patterns in real networks.

The entropy-degree diagram helps to visualize how the information is distributed across the network. The nodes with high entropy comprise more information. Their interactions into the networks are more “flexible”. That is, they are in a position where the diversity of interactions is arranged in a way that allows holding more information. The opposite can be affirmed to nodes with low entropy.

## B. Geodesic entropy of functional brain networks under Ayahuasca influence

We use the geodesic entropy to evaluate functional brain networks in different states of consciousness: ordinary state and psychedelic state induced by Ayahuasca. Ayahuasca is a sacred brew from Amazonian indigenous culture made with two plants from Amazonian flora – the leaves of the bush *Psychotria Viridis*, that contains N, N-Dimethyltryptamine (DMT), and the vine *Banisteriopsis caapi*, that contains monoamine oxidase inhibitors MAOi [6]. The DMT is a serotonergic psychedelic similar to LSD [16, 17], and mescaline but fast metabolized by the human body. The MAOi’s act slowing down this degradation, allowing the DMT to cross the blood-brain barrier and enabling hours of psychedelic experience [6]. For more information about Ayahuasca we refer to [18–22].

### 1. Data

The experimental procedures were performed in accordance with the guidelines and regulations approved by the Ethics and Research Committee of the University of São Paulo at Ribeirão Preto (process number 14672/2006). All volunteers sign a written informed consent. The fMRI data were acquired from 10 healthy adult volunteers (mean age 31.3, from 24 to 47 years, 5 women) with no history of neurological or psychiatric disorders – evaluated by DSM-IV structured interview [23]. They have at least 8 years of formal educational and minimum Ayahuasca use time of 5 years. They were in absence of any medication for at least 3 months prior to the acquisition and also had not take nicotine, caffeine, and alcohol prior to the acquisition. Each volunteer ingested about 120-200 mL (2.2 mL/kg of body weight) of Ayahuasca. The chromatography analysis detected on the brew 0.8 mg/mL of DMT, 0.21 mg/mL of harmine and no harmaline at the threshold of 0.02 mg/mL [24]. The volunteers were submitted to two sections of fMRI scanning: one before and other 40 minutes after Ayahuasca intake when the subjective effects can be observed. In both cases, volunteers were requested to be in an awake resting state, that is lying with their eyes closed, without performing any task. The samples of one volunteer were excluded from the dataset due to excessive head movement.

## 2. *Obtaining functional networks from fMRI data*

The methods to extract the networks from the fMRI data used here are the same performed in the reference [13]. The pre-processing of fMRI data was made according to standard guidelines. We performed spatial smoothing (Gaussian kernel, FWHM = 5 mm) and correction of slice-timing and head motion. We evaluated 9 regressors using a General Linear Model (GLM): 6 regressors to movement correction, 1 to white matter signal, 1 to cerebrospinal fluid and 1 to global signal [25]. The images were spatially normalized according to the Montreal Neurologic Institute (MNI152 template) anatomical standard space using a linear transformation. We evaluated the band-pass filter using maximum overlap wavelet transform (MODWT), considering the Daubechies wavelet to split the signal into 4 scales of distinct frequency bands. We choose the scale 3 (frequency band  $\approx 0.03 - 0.07$  Hz) to be in agreement with the literature that considers the low frequency ( $\approx 0.01$  to  $0.1$  Hz), preeminent on resting states [26].

We parcellate each image into 110 cortical anatomical regions according to the Harvard-Oxford cortical and subcortical structural atlas (threshold of  $> 25\%$ , using FMRIB software, an FSL library). We evaluated only 104 cortical regions because of an acquisition limitations for some subjects. The cortical regions were used to define the nodes of the brain networks and the correlation between their signals to define the links. The signals corresponding to each cortical region were obtained averaging the time series of all voxels (3D regular grid) into them (using Marsbar, SPM toolbox). We calculate the Pearson correlation of temporal series of all possible pairs of cortical regions, yielding a cross-correlation matrix. Thus, we have for each sample (before and after Ayahuasca of all subjects) a  $104 \times 104$  correlation matrix considered as an estimative of the brain functional connectivity. Since the cortical regions define the nodes, the correlation matrices were used to define the links of the functional brain networks.

For each sample, we generated a set of symmetric binary adjacency matrices by thresholding the absolute value of their correlation matrices. Precisely, whether the absolute value of the element matrix is larger than the defined threshold, a link is formed ( $A_{i,j} = 1$ ), otherwise, no link is formed ( $A_{i,j} = 0$ ). We choose a range of thresholds that ensure the networks were fully connected but also sparse. We adopted the same criteria of references [13, 27–29]. We consider the network with lower global efficiency and greater local efficiency than its

randomized version [30]. We fixed the same band of thresholds for all samples, allowing a more accurate comparison. It was necessary to exclude two subjects from our analysis due to a trade-off in the range, leaving 7 subjects (4 women). As long as we intend to evaluate the difference between topological features of networks before and after Ayahuasca intake, we compare networks with the same density of links. The chosen threshold correlation range is  $0.28 \leq \eta \leq 0.37$  that yield networks with mean degree in the range  $24 \leq \langle k \rangle \leq 39$ . Summarizing, we created two sets of networks (before and after Ayahuasca intake) that allow 16 different comparisons (i.e. of differing mean degrees) for each subject’s sample. The reader can find further details in the reference [13].

### III. RESULTS

Figure 4 shows the entropy-degree diagram of one of the subjects before and after Ayahuasca intake for networks with mean degree  $\langle k \rangle = 25$  and  $\langle k \rangle = 32$ . Note that the nodes in the entropy-degree diagram after Ayahuasca tend to have higher entropy. All subjects presented similar behavior. See supplementary material. Figure 5 shows the divergences of the characteristic geodesic entropies between after and before Ayahuasca for each subject by comparing pair of networks with the same density of links. The boxplot depicts the distribution of characteristic geodesic entropy differences ( $\Delta S^g = S_{after}^g - S_{before}^g$ ) of networks with the same mean degree. Note the characteristic geodesic entropy increases for all subjects after Ayahuasca intake. Figure 6 shows the contrast of the characteristic geodesic entropy of networks with the same mean degree (same densities of links) averaged over all subjects before (blue) and after (brown) Ayahuasca intake. The increasing also appear in this graphic suggesting that characteristic geodesic entropy of functional networks under Ayahuasca influence tends to be higher than in ordinary condition.

The black and gray curves show the characteristic geodesic entropy for the randomized versions of the networks before and after Ayahuasca respectively. We used the Maslov algorithm [30] to randomize the links of networks keeping their degree distribution unchanged. In other words, the Maslov randomization breaks all structural trends that do not depend on the degree distribution. Note that the randomization reduces the entropy in both conditions and no considerable divergence was found between the randomized curves. These results mean that the change in geodesic entropy we detected before and after Ayahuasca intake is

related to underlying trends of the network structure. They do not result from the known changes in degree distribution [13].

#### IV. DISCUSSION AND CONCLUSION

The (often non-trivial) rules of interactions among the nodes of a network determine the nature of its emergent behaviors. In many cases, the network interactions are defined by the relative position of each node in the network structure. The role of a node in a network depends on how it is contextualized inside the network. In a highly connected network, a node does not interact only with its first neighbors, but also interact indirectly with the other nodes. The geodesic entropy quantifies the statistics (i.e. the the entropy functional of the probability distribution) of the geodesic distances from a given node to all other nodes in the network, by classifying all nodes according to their neighborhood radii.

In summary, we evaluate the geodesic entropy of functional brain network of subjects in the resting state before and after the ingestion of the psychedelic brew Ayahuasca. We find that nodes of the functional network during Ayahuasca experience tends to have greater geodesic entropy than in the ordinary condition, resulting in networks with higher characteristic geodesic entropy. Hence, the geodesic distances between nodes become less constrained on average, i.e. their distribution becomes “wider.” In a previous work, we showed that the entropy of the degree distribution of brain functional connectivity networks under the influence of Ayahuasca is greater than in the ordinary state [13]. The entropy of degree distribution is a global measurement and networks with different patterns can share the same degree distribution. The result presented in this paper suggests that the patterns can be less restricted under Ayahuasca influence than in ordinary condition and it does not depend on the degree distributions. The diversity of geodesic distances are more well-distributed contributing to the flexibility of interaction of the networks.

The hypothesis of entropy increases in some aspect of brain in psychedelic states has been discussed in the literature [31–33]. This entropic brain hypothesis predicts that the psychedelics state is associated with greater entropy compared to the ordinary state. The hypothesis could explain the increased flexibility in thoughts, facility to access suppressed memory, increase of creativity, among others [31].

In conclusion, we have shown how the geodesic entropy quantifies locally the connectivity

to the network globally. Further, we have used entropy-degree diagrams to evaluate the role of each node in the network, giving a clearer view of the network topology and global connectivity. The application to fMRI-based functional connectivity networks sheds insights on how the brain changes under the influence of external influences. In this study, we used Ayahuasca, but there is no reason why the method could not be applied to a variety of drugs or meditative states, etc. We hope that these ideas and methods find use in furthering our understanding of complex networks in general and in brain function networks specifically.

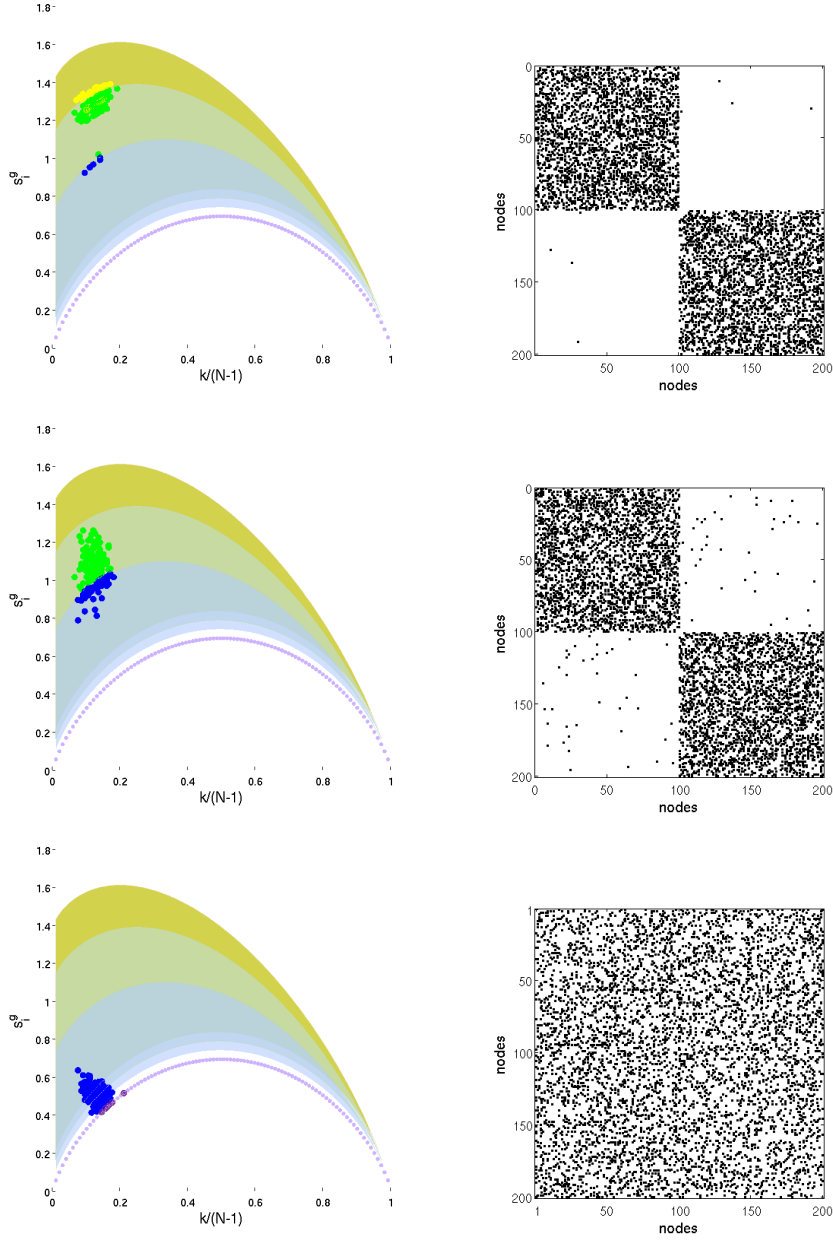


Figure 2. Illustration of entropy-degree diagram for three different artificially generated networks with the same number of nodes, links, same degree distribution ( $\langle k \rangle = 25$ ), but different structural configurations. On the right side of each entropy-degree diagram is the adjacency matrix of the corresponding network. The characteristic geodesic entropy are  $S^g = 1.26$  nats,  $S^g = 0.98$  nats,  $S^g = 0.52$  nats respectively from panels up to down. The colors purple, blue, green and red are defined according to the maximum neighborhood radius  $r_{max} = 2, 3, 4$  and  $5$ . The watermark regions delimit the space of possibilities for each value of the maximum neighborhood. The minimum entropies possible are delimited by the purple curve and depends on the node degree.

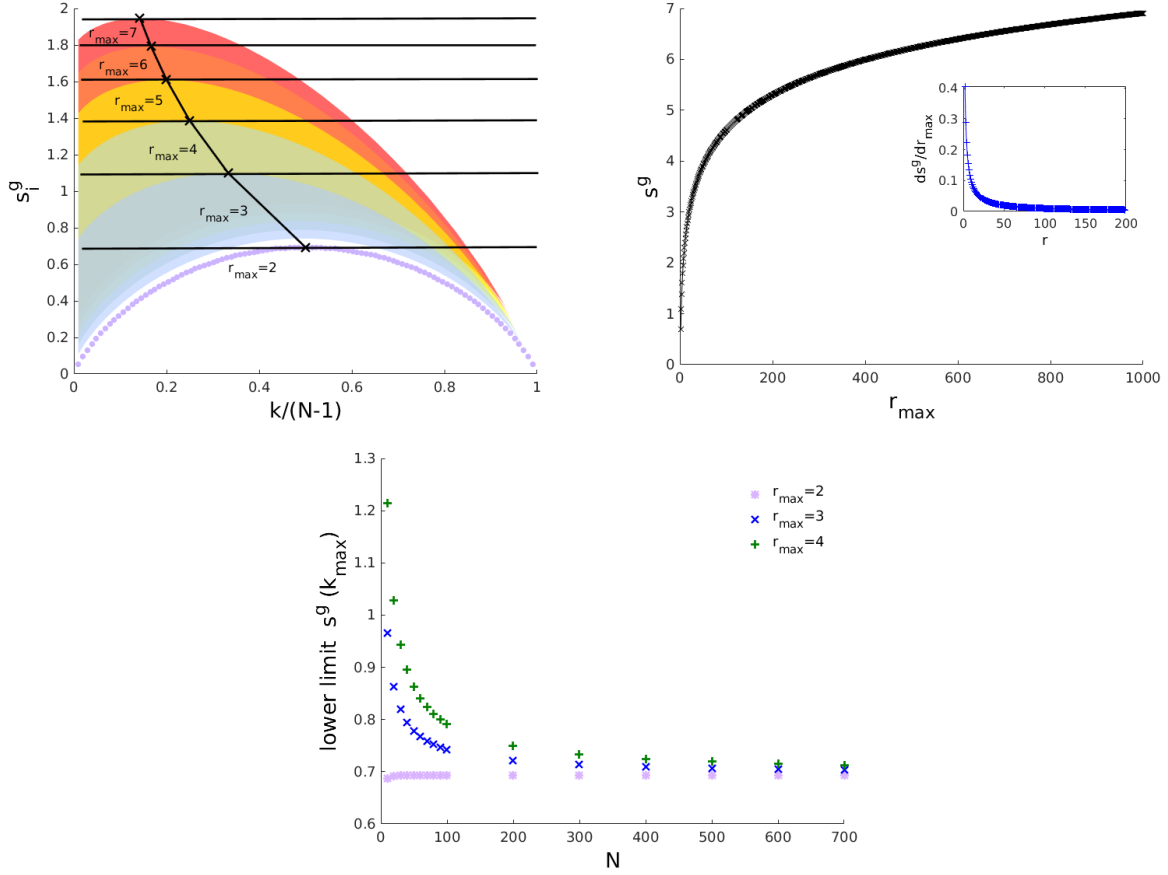


Figure 3. Universal relations for geodesic entropy. In the  $sk$ -diagram on left, the colored regions delimit the regions of nodes with maximum neighborhood values ( $r_{max}$ ) indicated by the labels. The maximum value of each region is in  $s_i^g \approx \ln(r_{max})$ , that correspond to  $k \approx 1 \setminus r_{max}$ . The middle plot shows the variance in the maximum entropy due the increase of neighborhood radius  $r_{max}$ . Its increases are inversely proportional to  $r_{max}$  ( $\Delta s_{max}^g \approx r_{max}^{-1} \Delta r_{max}$ ). Note that for small values of  $r_{max}$ , its increasing will result in an increase in contribution to the entropy. Nevertheless, for large  $r_{max}$  the contribution does not change significantly. Note that none of these values depend on network size. The finite size effect appears in the lower limit. For large networks, all regions will be delimited within the first curve ( $r_{max} = 2$ ). The lower limit will depend on the network size for finite networks. The right plot shows the influence of the network size in the lower limits.

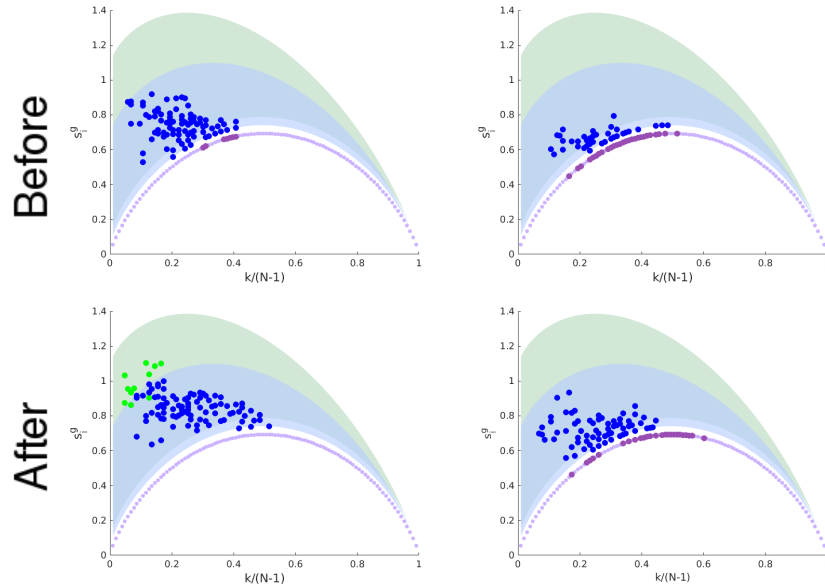


Figure 4. entropy-degree diagram before and after Ayahuasca. The panels depict the entropy-degree diagrams for one of the subjects before (upper row) and after (bottom row) Ayahuasca intake for networks with mean degree  $\langle k \rangle = 25$  and  $\langle k \rangle = 32$  respectively. The colors follow the same rules of figure 2. Note the nodes after Ayahuasca tends to occupy populate regions in the diagram of higher entropy.

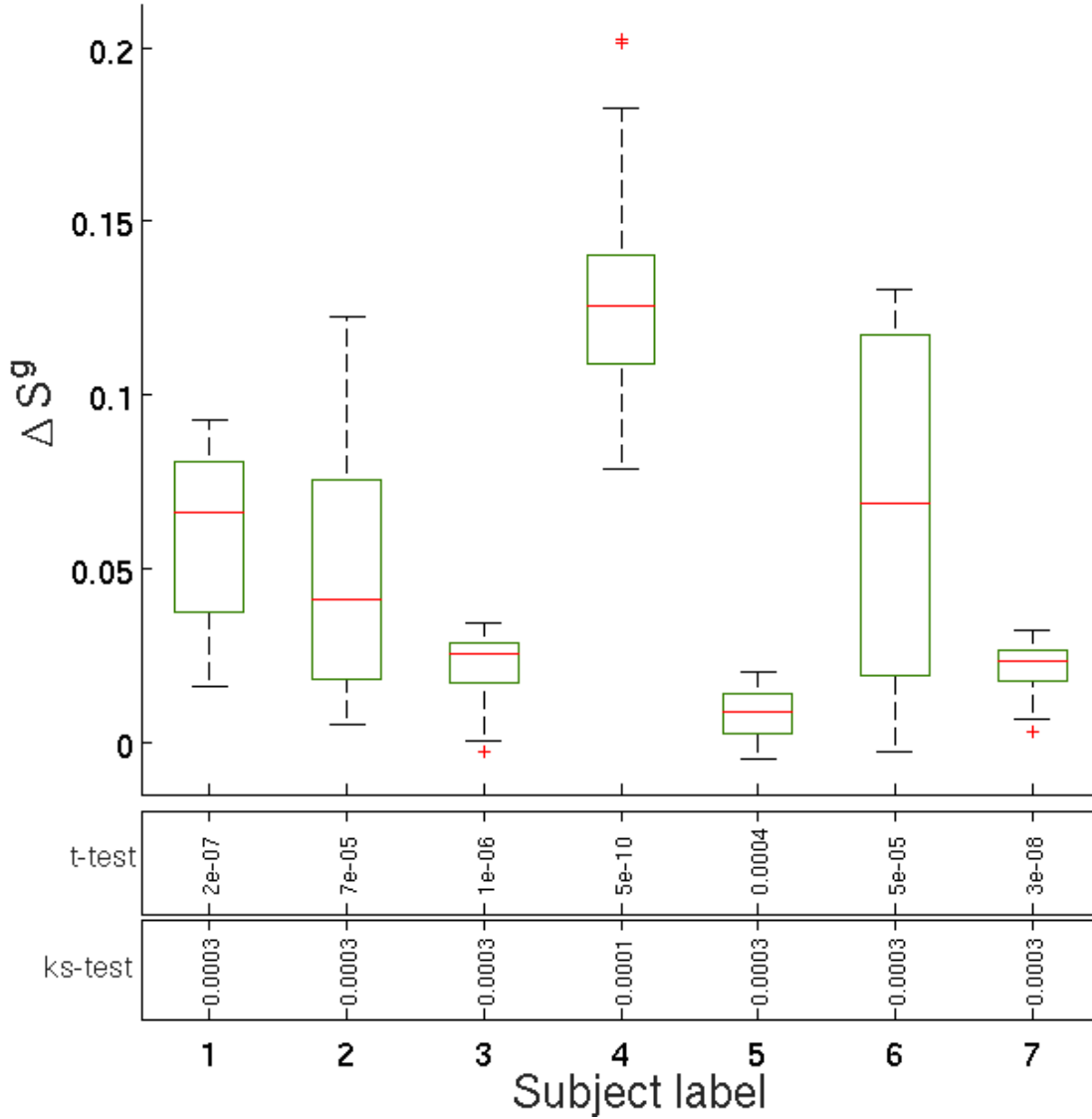


Figure 5. Nodal entropy before and after Ayahuasca. The boxplot shows the averaged geodesic entropy in 16 networks with the mean degree from  $\langle k \rangle = 24$  to  $\langle k \rangle = 39$  for each subject before (blue) and after (green) Ayahuasca. The median value increases for all of them.

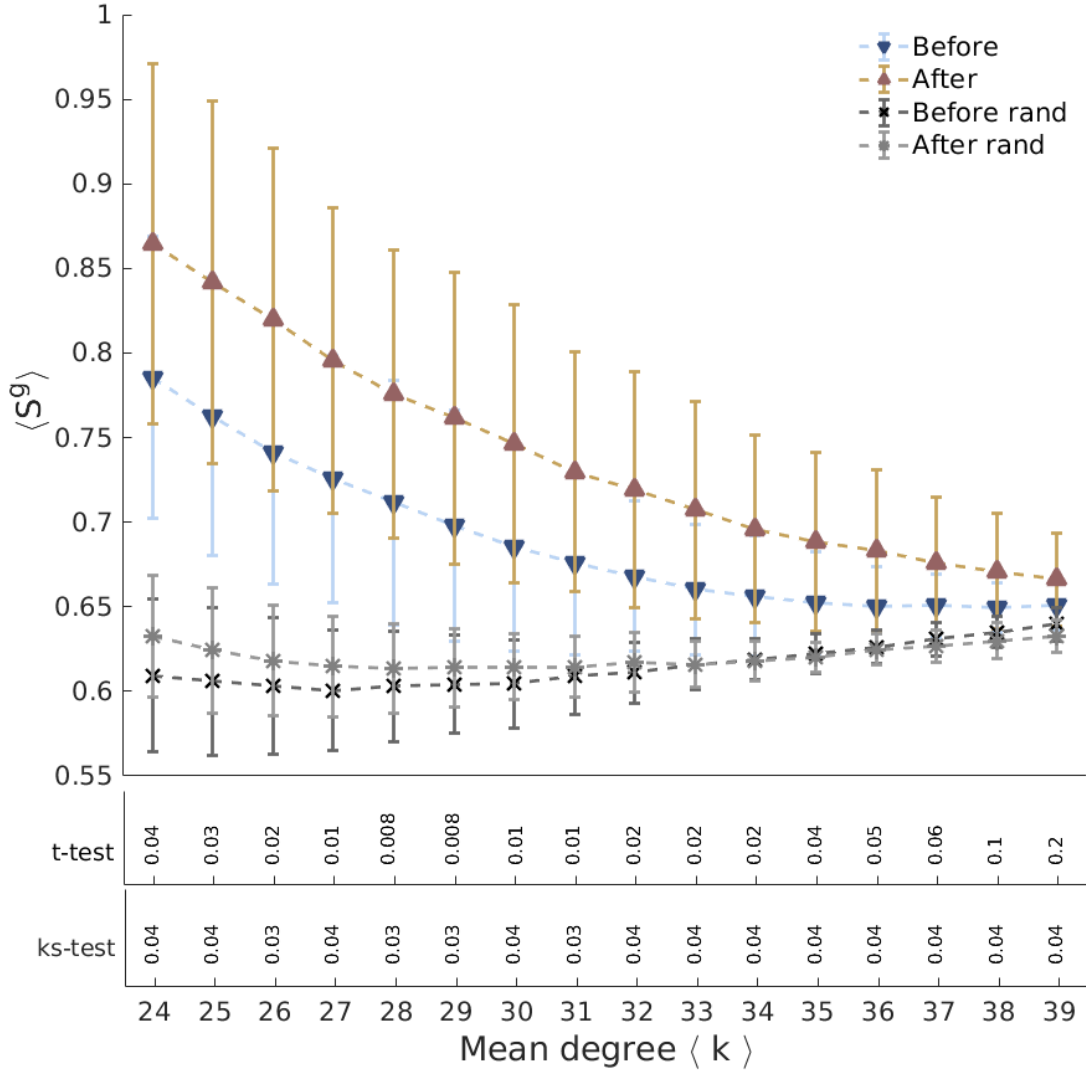


Figure 6. Mean geodesic entropy before and after Ayahuasca. The graphic shows the mean geodesic entropy under all subjects for before and after Ayahuasca for networks with different densities (mean the degree from  $\langle k \rangle = 24$  to  $\langle k \rangle = 39$ ). The mean geodesic entropy is greater for all networks densities.

## V. SUPPLEMENTARY INFORMATION

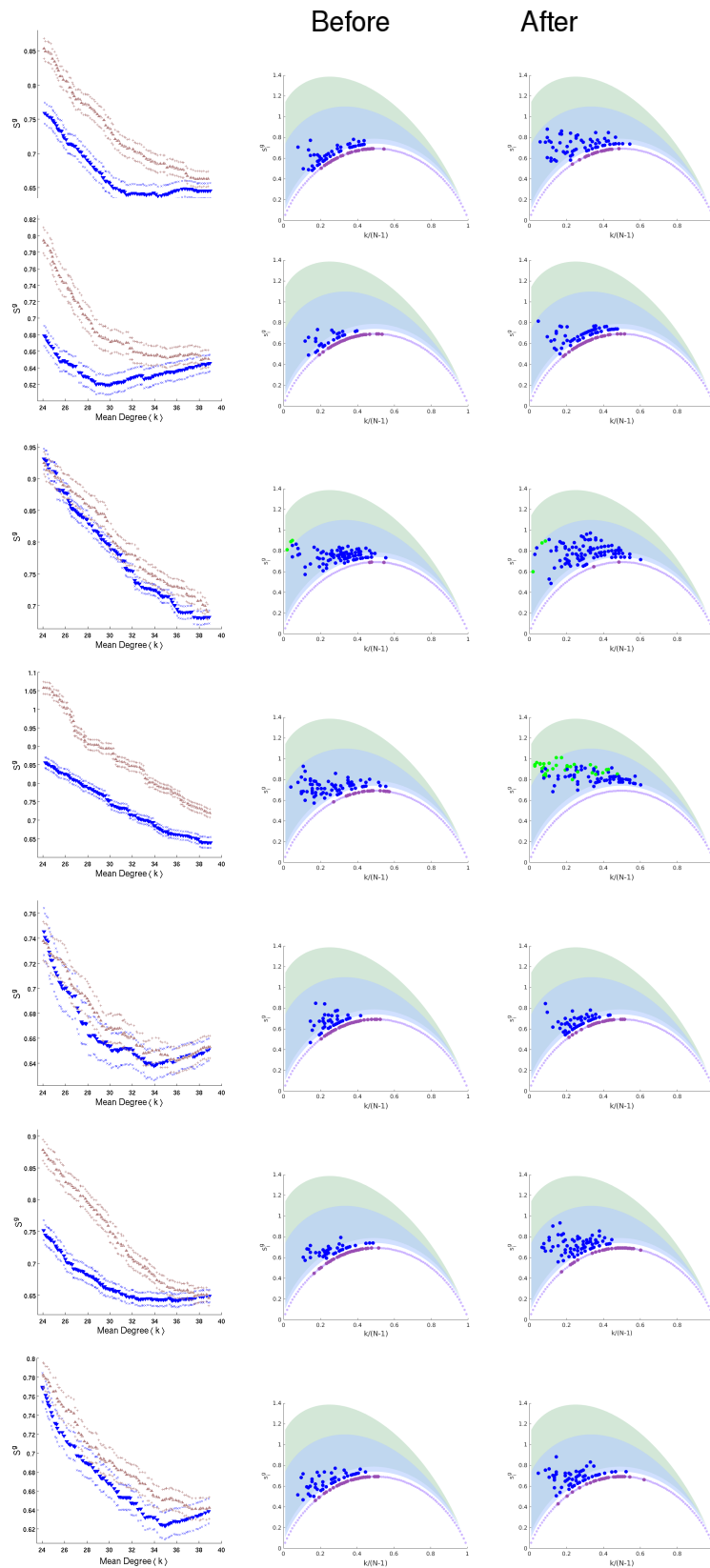


Figure 7. Geodesic entropy before and after Ayahuasca intake for all subjects. The first column depicts the curves to characteristic geodesic entropy for networks with the mean degree from  $\langle k \rangle = 24$  to  $\langle k \rangle = 39$  for before (blue) and after (brown) Ayahuasca intake. The second and third columns show the sk-diagram for before and after respectively ( networks with mean degree  $\langle k \rangle = 32$  ). Note an increase of geodesic entropy for all subjects.

- 
- [1] J. D. Haynes and G. Rees, *Nat. Rev. Neurosci.* **7**, 523 (2006).
- [2] M. E. J. Newman, *Social Networks* 2005 **27**, 39 (2005).
- [3] M. P. van den Heuvel and O. Sporns, *Trends Cogn. Sci.* **17**, 683 (2013).
- [4] B. Hou, Y. Yao, and D. Liao, *Physica A: Statistical Mechanics and its Applications* **391**, 4012 (2012 2012/0).
- [5] C. E. Shannon, *The Bell System Technical Journal* **27**, 379 (July 1948).
- [6] J. Riba, M. Valle, G. Urbano, M. Yritia, A. Morte, and M. J. Barbanoj, *Journal of Pharmacology and Experimental Therapeutics J Pharmacol Exp Ther* **306**, 73 83 10.1 (2003).
- [7] B. Shanon, *Antipodes of the Mind* (Oxford University Press UK, 2002).
- [8] R.-F. A. U. G. Riba, J., A.-R. M. M. C. J. C. Morte, A., and M. J. Barbanoj, *Psychopharmacology* **154**, 85 (2001 2001/0).
- [9] M. E. J. Newman, *Networks: an introduction* (Oxford University Press, Inc., New York, 2010).
- [10] R. Albert and A. L. Barabasi, *Rev. Mod. Phys.* **74**, 47 (2002).
- [11] M. Rubinov and O. Sporns, *NeuroImage* **52**, 1059 (2010).
- [12] D. J. Watts and S. H. Strogatz, *Nature* **393**, 440 (1998).
- [13] A. Viol, F. Palhano-Fontes, H. Onias, D. B. de Araujo, and G. M. Viswanathan, *Sci. Rep.* **7**, 7388 (2017).
- [14] Z. Chen, *IEEE Trans. Control Network Syst.* **1**, 349 (2014).
- [15] M. Stella and M. De Domenico, *Entropy* **20** (2018).
- [16] A. Hofmann, J. Ott, and A. Feilding, *LSD: My Problem Child* (OUP Oxford, 2013).
- [17] T. Passie, J. H. Halpern, O. D. Stichtenoth, H. M. Emrich, and A. Hintzen, *CNS Neur. & Ther.* **14**, 295 (2018).
- [18] B. Shanon, *The Antipodes of the Mind: Charting the Phenomenology of the Ayahuasca Experience* (Oxford University Press, 2002).
- [19] B. C. Labate and C. Cavnar, *Ayahuasca Shamanism in the Amazon and Beyond*, Oxford Ritual Studies Series (Oxford University Press, 2014).
- [20] B. C. Labate and C. Cavnar (Springer-Verlag, 2014).
- [21] B. C. Labate and C. Cavnar, *The Therapeutic Use of Ayahuasca* (Springer-Verlag, 2013).

- [22] J. Riba, A. Rodriguez-Fornells, G. Urbano, A. Morte, R. Antonijoan, M. Montero, C. J. Callaway, and J. M. Barbanøj, *Psychopharmacology* **154**, 85 (2001).
- [23] A. P. Association and A. P. A. T. F. on DSM-IV., *Diagnostic and Statistical Manual of Mental Disorders: DSM-IV-TR*, Diagnostic and Statistical Manual of Mental Disorders: DSM-IV-TR (American Psychiatric Association, 2000).
- [24] D. B. De Araujo, S. Ribeiro, G. A. Cecchi, F. M. Carvalho, T. A. Sanchez, J. P. Pinto, B. S. de Martinis, J. A. Crippa, J. E. C. Hallak, and A. C. Santos, *Human Brain Mapping* **33**, 2550 (2012).
- [25] We used FSL Software, a free library of statistical tools available by Oxford Centre for Functional MRI of the Brain (<http://www.ndcn.ox.ac.uk/divisions/fmrib>).
- [26] P. Fransson, *Human Brain Mapping* **26**, 15 (2005).
- [27] H. Onias, A. Viol, F. Palhano-Fontes, K. C. Andrade, M. Sturzbecher, G. Viswanathan, and D. B. de Araujo, *Epilepsy & Behavior* **38**, 71 (2014).
- [28] M. S. Schroter, V. I. Spoormaker, A. Schorer, A. Wohlschlager, M. Czisch, E. F. Kochs, C. Zimmer, B. Hemmer, G. Schneider, D. Jordan, and R. Ilg, *Journal of Neuroscience* **32**, 12832 (2012).
- [29] Y. Liu, M. Liang, Y. Zhou, Y. He, Y. Hao, M. Song, C. Yu, H. Liu, Z. Liu, and T. Jiang, *Brain* **131**, 945 (2008).
- [30] S. Maslov and K. Sneppen, *Science* **296**, 910 (2002).
- [31] R. Carhart-Harris, R. Leech, P. J. Hellyer, M. Shanahan, A. Feilding, E. Tagliazucchi, D. R. Chialvo, and D. Nutt, *Frontiers in Human Neuroscience* **8**, 20 (2014).
- [32] D. Papo, *Frontiers in Human Neuroscience* **10**, 423 (2016).
- [33] R. L. Carhart-Harris, *Neuropharmacology* (2018).